Electronic Supplementary Material (ESI) for Soft Matter.
This journal is © The Royal Society of Chemistry 2024

Electronic Supplementary Information:

Highly Flexible PEG-LifeAct Constructs act as Tunable Biomimetic Actin Crosslinkers

Tyler D. Jorgenson[1], Kashmeera D. Baboolall[2], Cristian Suarez[3], David R. Kovar[3,4], Margaret L. Gardel[1,5,6,7], Stuart J. Rowan[1,8]

[1]Pritzker School of Molecular Engineering, [2]Graduate Program in Biophysical Sciences, [3]Department of Molecular Genetics and Cell Biology, [4]Department of Biochemistry and Molecular Biology, [5]Institute for Biophysical Dynamics, [6]James Franck Institute, [7]Department of Physics, [8]Department of Chemistry

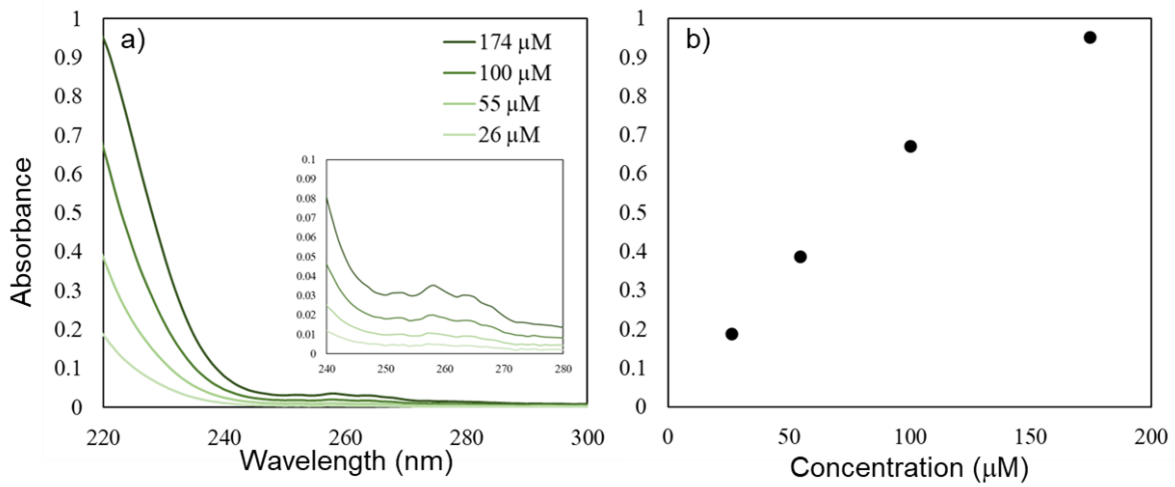

Figure S1. a) Full UV-Vis absorbance of azido-hexanoic acid functionalized LifeAct peptides showing the dominant absorption of the peptide backbone at 220 nm. Absorbance values at 220 nm were used to construct a calibration curve for the concentration determination of the PEG-LifeAct constructs. Inset highlights the subtle phenylalanine absorbance at the expected wavelength of 257 nm was used to determine the concentration of the azide functionalized LifeAct and calibrate the 220 nm calibration curve. b) Calibration curve for LifeAct for absorbance at 220 nm showing slight non-linearity above 100 micromolar of LifeAct. All PEG-LifeAct constructs were determined within the linear regime with the calculated molar extinction coefficient of 6500 ± 180 M^{-1} cm^{-1}.

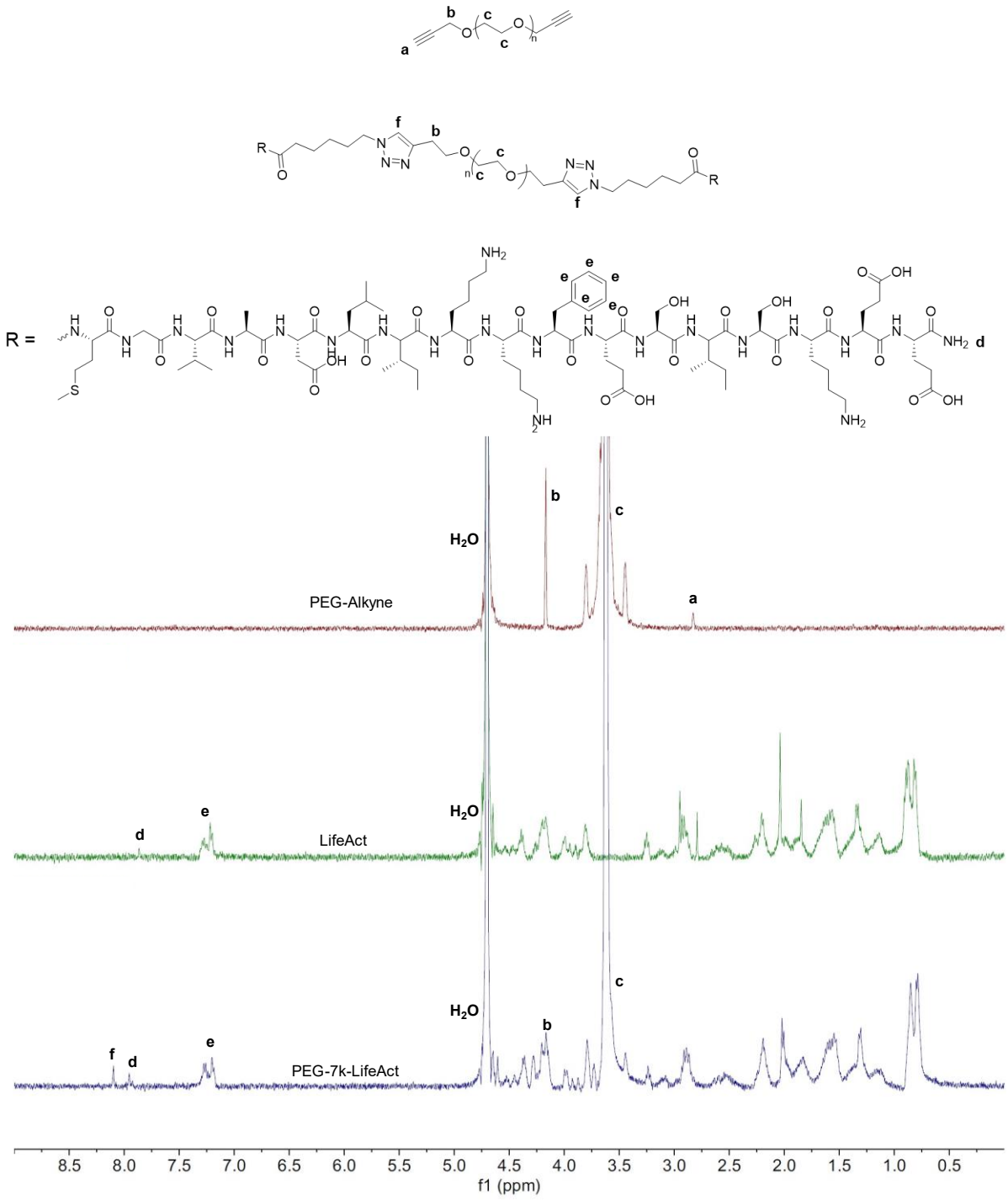

Figure S2. (top) Chemical structure of PEG-Alkyne and LifeAct functionalized PEG. (bottom) Corresponding nuclear magnetic resonance spectrum with key protons labelled. Complete functionalization of the PEG was confirmed by the presence of the triazole proton (f), the disappearance of the alkyne proton (a), and the expected ratio between the phenylalanine protons (e) and PEG backbone protons (c).

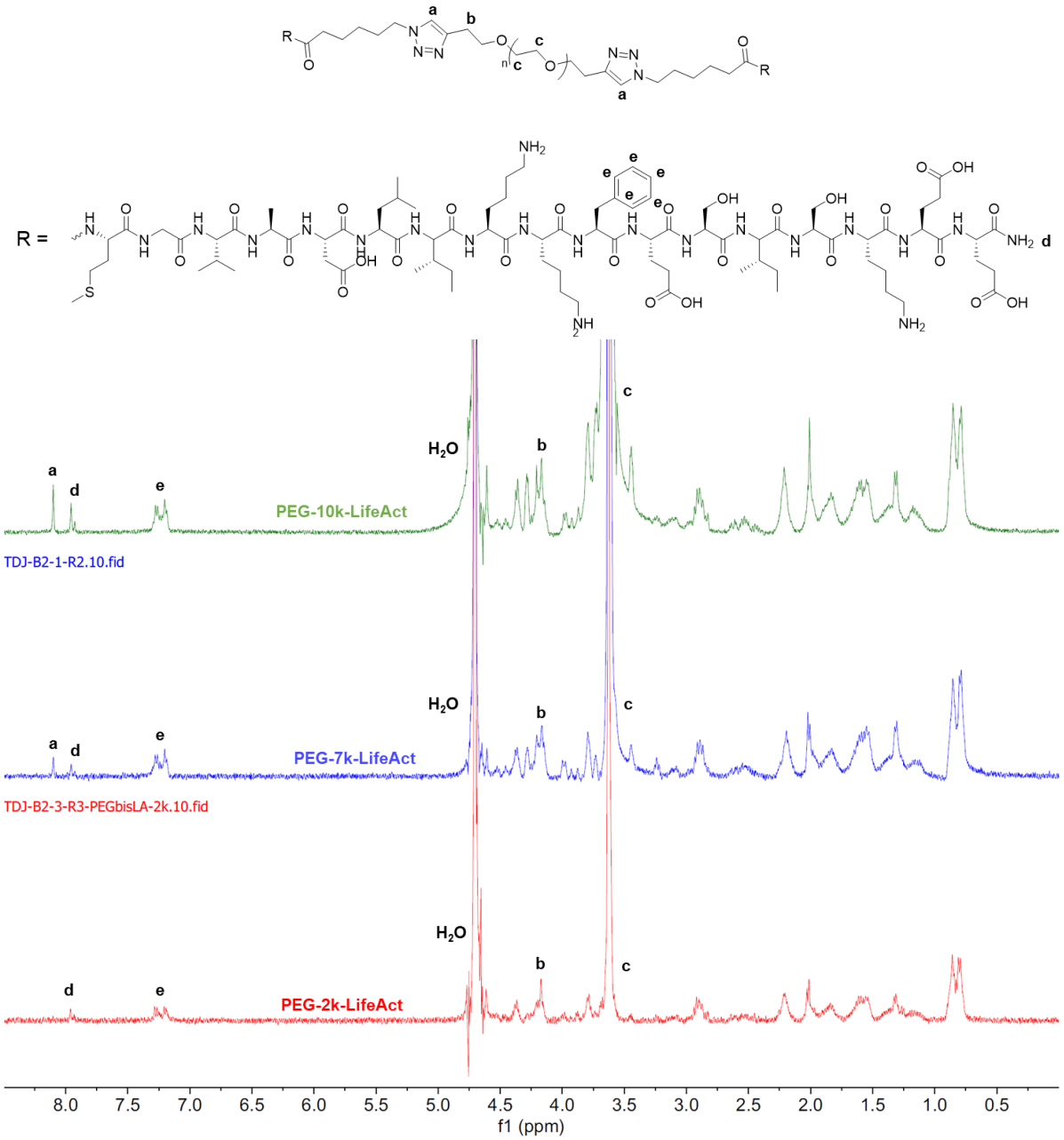

Figure S3. Nuclear magnetic resonance (NMR) spectrum of each PEG-LifeAct construct showing the pertinent protons for determining polymer functionality. Namely, the ratio of phenylalanine protons (e) to PEG backbone protons (c). Less than 1 milligram of product was used for the NMR spectrum for PEG-2k-LifeAct due to the smaller total molecular weight (~6kDa) leading to significant loss during purification via centrifugal filtration. As a result, the triazole peak is not visible in the NMR spectrum. Expected ratio between (e) and (c) in addition to the lack of residual alkyne peaks suggests the PEG-2k-LifeAct construct is well functionalized.

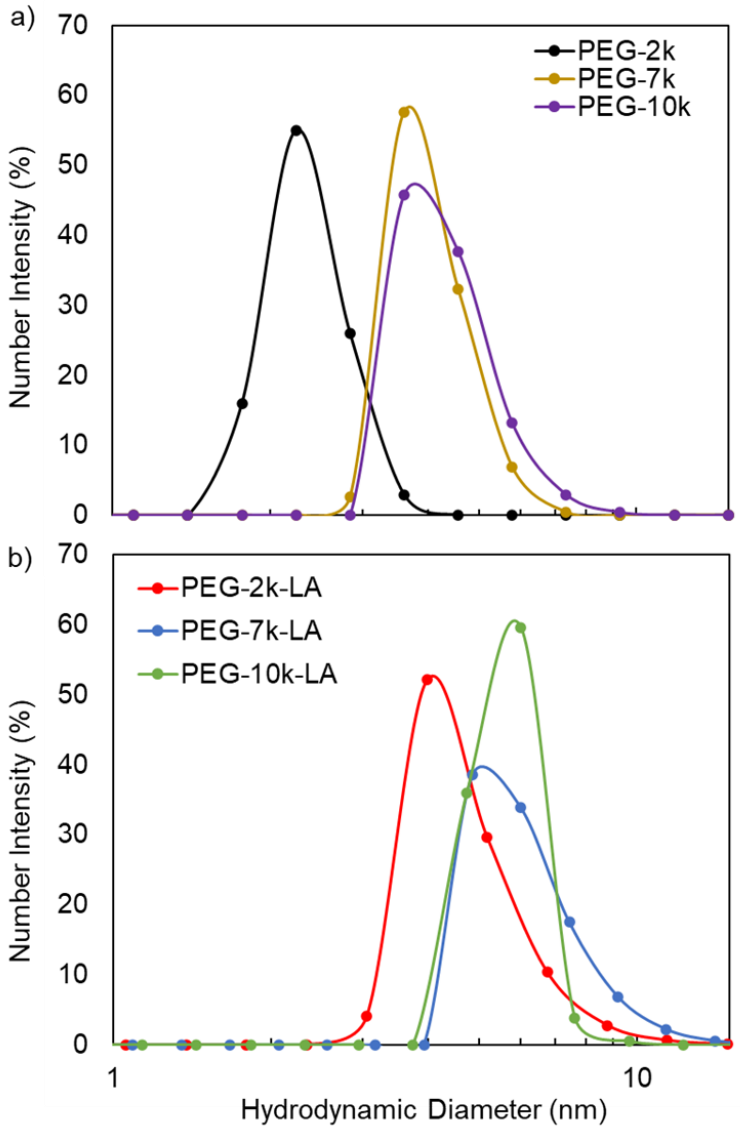

Figure S4. (a) Number intensity dynamic light scattering of PEG-Alkynes with molecular weights of 2k, 7k, and 10kDa in calcium buffer at 25°C showing diameters of approximately 2.5, 4, and 4 nanometers, respectively. (b) DLS of PEG-LifeAct constructs in calcium buffer at 25°C showing the hydrodynamic diameter. All constructs had a consistent 2 nanometer increase in hydrodynamic diameter when compared to their unfunctionalized counterparts suggesting the attachment of the LifeAct peptide. PEG-LifeAct constructs had diameters of approximately 5 to 6 nanometers.

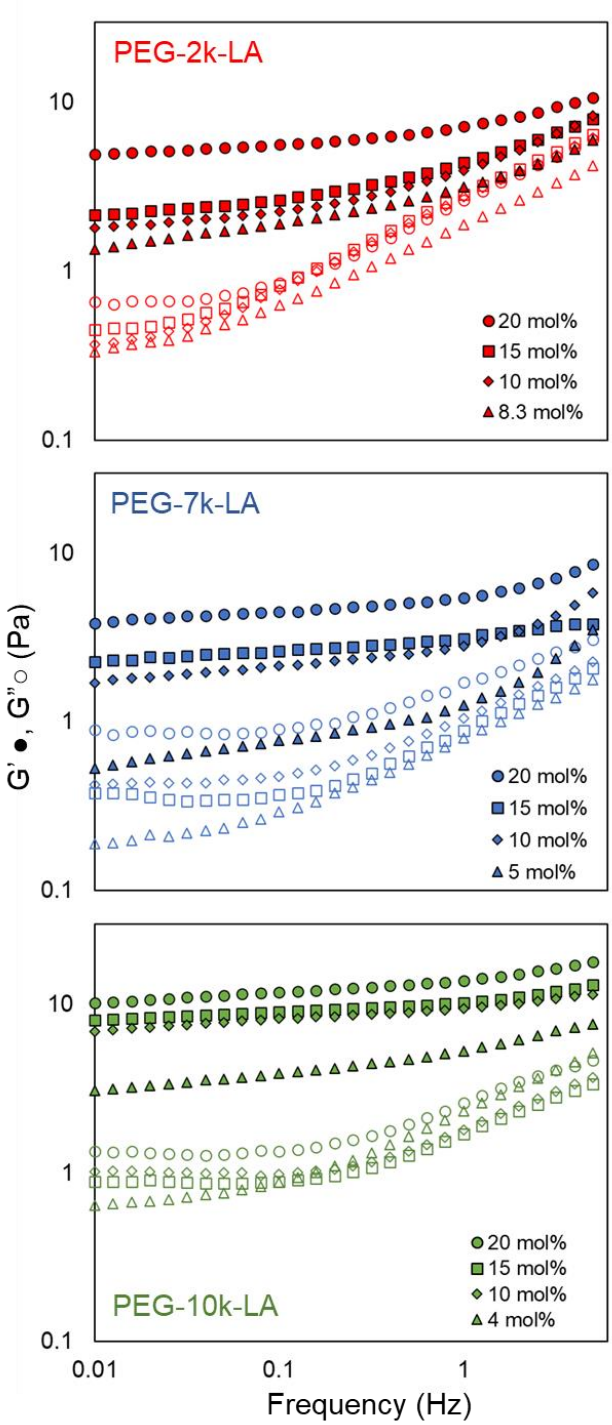

Figure S5. Representative frequency sweeps of PEG-2k-LA, PEG-7k-LA, and PEG-10k-LA above their respective critical concentrations for actin concentration of 23.8 μM.

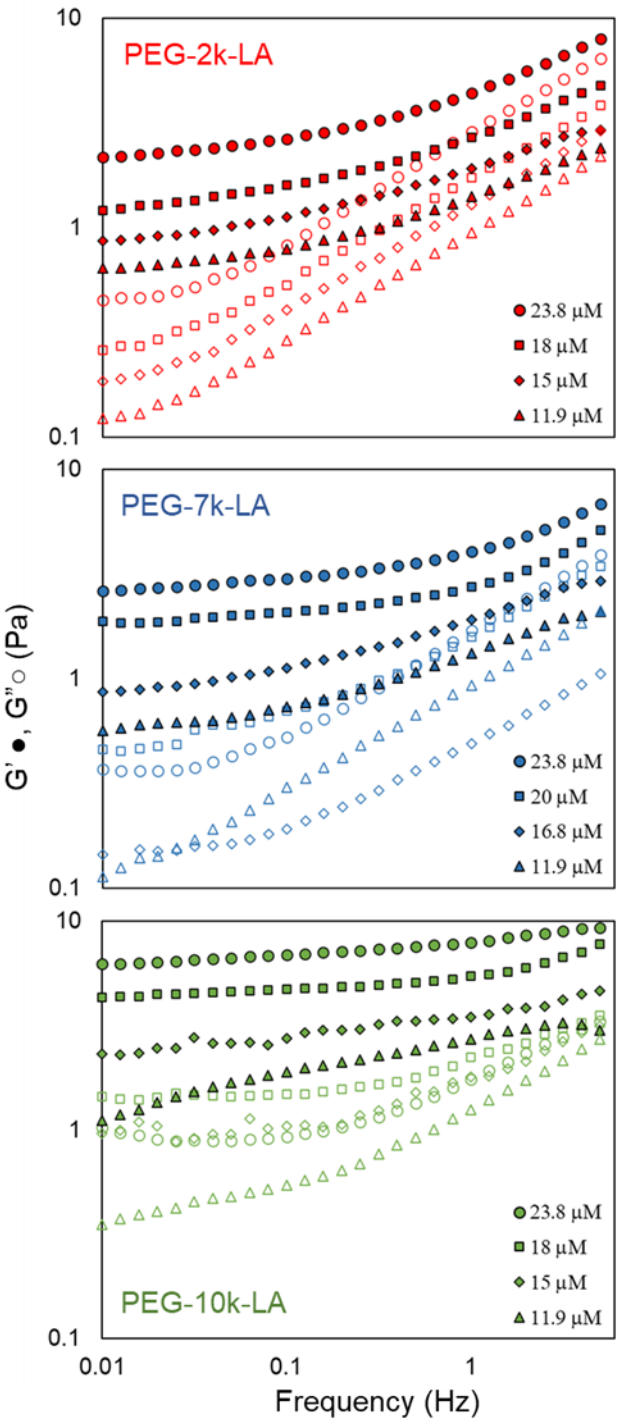

Figure S6. Representative frequency sweeps of PEG-2k-LA, PEG-7k-LA, and PEG-10k-LA at 15 mol% for increasing actin concentration from 11.9 μM to 23.8 μM.

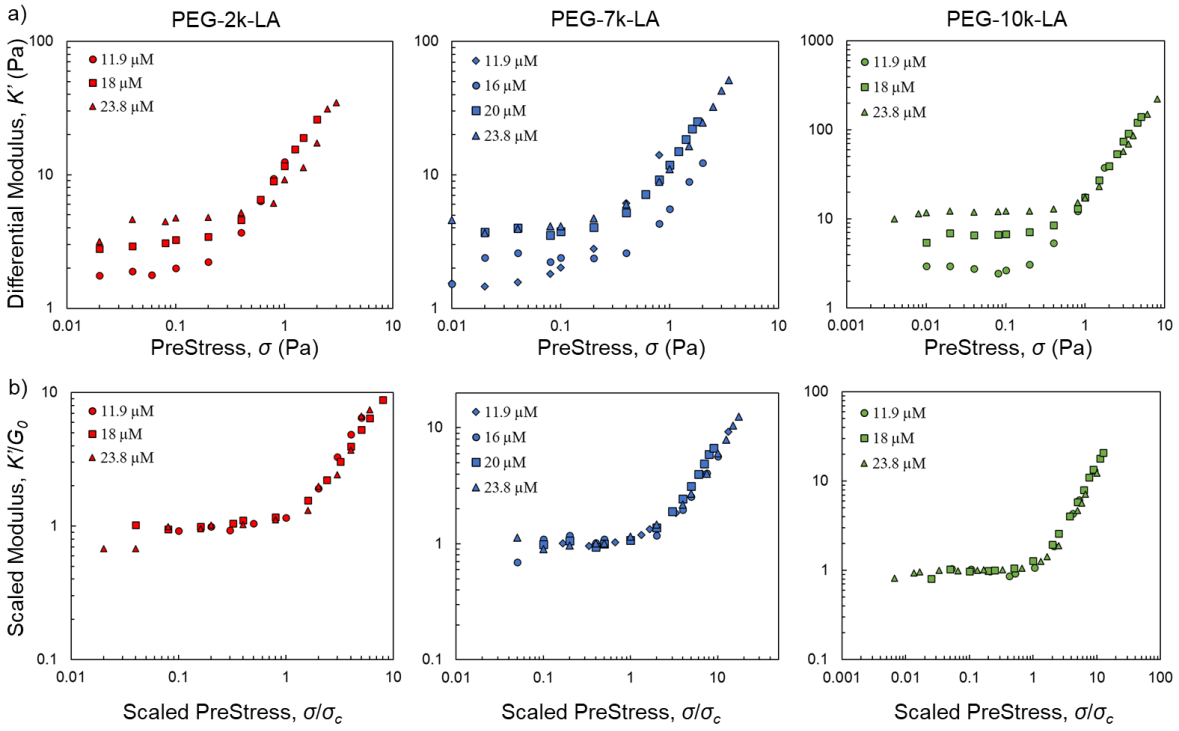

Figure S7. a) Representative stress-stiffening curves for PEG-LifeAct constructs at 15 mol% crosslinker and variable concentrations of actin. b) Scaling the stress-stiffening curves presented in (a) with their respective critical stress and plateau modulus yields master curves with a single stress stiffening power law.

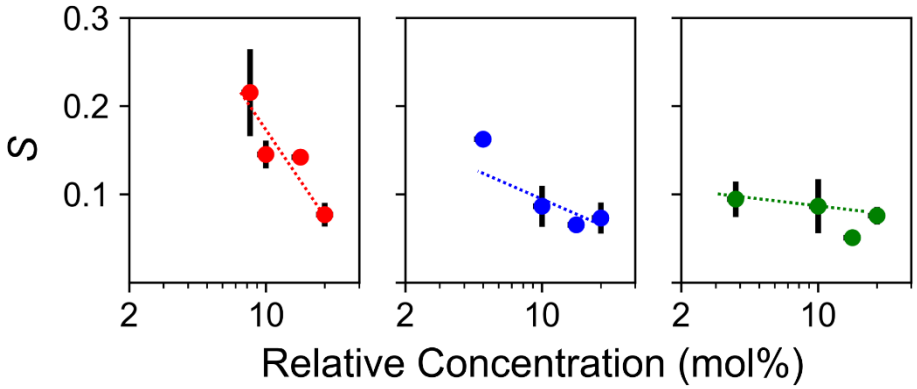

Figure S8. Average steepness of PEG-LA network frequency dependence determined from a power law fit of G' from 0.01 to 1 Hz for PEG-2k-LA (red), PEG-7k-LA (blue), and PEG-10k-LA (green). The y-axis error bars are for N=3. X-axis error bars are propagated from concentration errors based on UV measurements of the actin and crosslinker concentrations. Actin concentration was 23.8 μM for all networks.

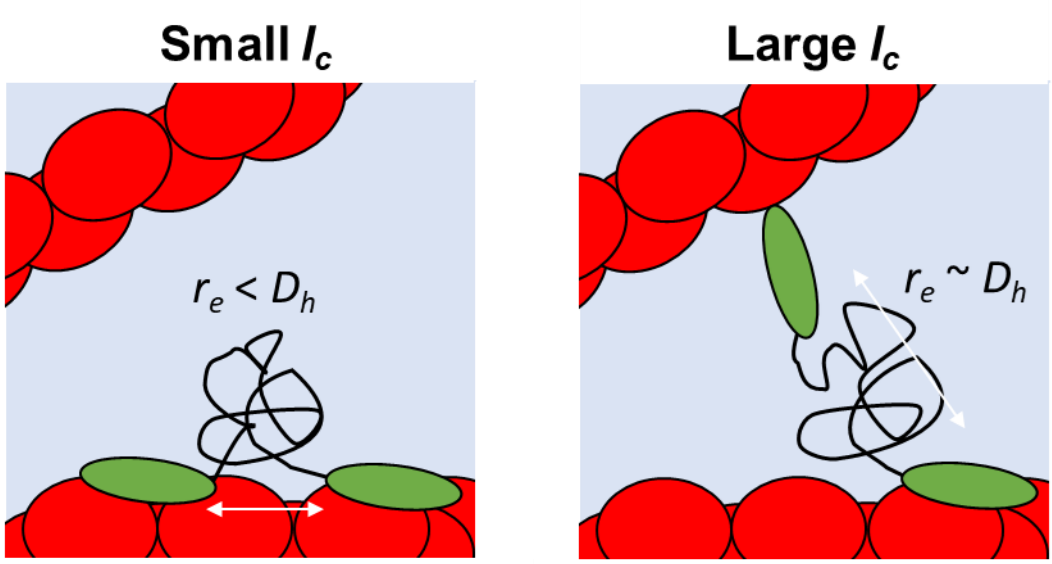

Figure S9. Schematic describing anticipated structural differences between small and large contour length, l_c, PEG-LA constructs. For small l_c constructs the chain end-to-end distance, r_e, (white arrows) is smaller than the hydrodynamic diameter, D_h, forcing the LifeAct binding domains to be in close proximity. For larger l_c constructs, the average r_e is equivalent to D_h ensuring effective positioning of LifeAct for crosslinking F-actin filaments.

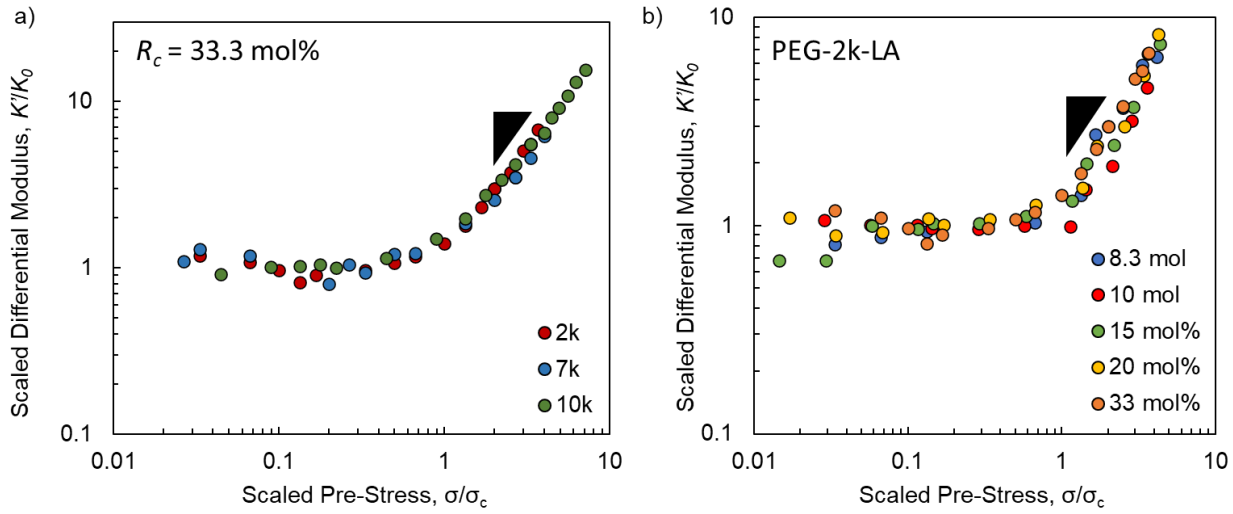

Figure S10. (a) Stress stiffening properties of PEG-LA with different PEG molecular weights at R_c = 33.3 mol% showing the same 3/2 power law (black triangle inset) predicted for thermal affine networks. (b) Stress-stiffening behavior of PEG-2k-LA for different R_c above R_c* showing the same power law holds.

Note S1: Under small deformations, PEG is well described by an entropic spring in which the force required to straighten the chain is related to the change in end-to-end distance of the polymer according to the following relationship:

$$F = -\frac{3k_bT}{2l_cl_p}\Delta r_{ee}$$

In which l_p is the persistence length, l_c is the contour length, k_b is the Boltzmann constant, T is the temperature in Kelvin, and r_{ee} is the end-to-end distance. Thus, the effective spring constant is:

$$k_{eff} = \frac{3k_bT}{2l_cl_p}$$

For effective spring constants presented in the Table 1, we assumed k_BT = 4.1 pN nm, l_p = 0.37 nm, and contour lengths of 13, 45, and 65 nm for the 2k, 7k, and 10k, respectively.

Note S2: For an ideal chain, the end-to-end distance r_e is defined as:

$$r_e = \sqrt{\frac{8}{3\pi} < r_e^2 >} = \sqrt{\frac{8}{3\pi} b^2 N}$$

Where $<r_e^2>$ is the mean squared end-to-end distance, b is the persistence length, and N is the number of segments in the polymer. Assuming b = 0.37 nm, N_{2k} = 45, N_{7k} = 160, and N_{10k} = 227, the expected re for the PEG-LA constructs are 2.3, 4.4, and 5.3 nm for the 2k, 7k, and 10k constructs, respectively. The following table outlines collects the r_e and D_h for the PEG-LA constructs.

Construct Name	r_e	D_h	r_e/D_h
PEG-2k-LA	2.3	4.7 ± 1.7	0.48 ± 0.17
PEG-7k-LA	4.4	6.2 ± 1.5	0.71 ± 0.17
PEG-10k-LA	5.3	5.6 ± 0.7	0.94 ± 0.12

Assuming the inner-LifeAct distance is well approximated by r_e, a r_e significantly smaller than D_h requires the chain ends to be on the same "side" of the globular PEG-LA construct (See Supplementary Figure 9). This is the case for PEG-2k-LA. PEG-7k-LA and PEG-10k-LA have comparable r_e and D_h suggesting a large proportion of the constructs display LifeAct domains on near opposite sides of the globular PEG chain. Close proximity of the LifeAct domains in PEG-2k-LA may impede bridging between F-actin and thus prevent effective crosslinking and bundling. The ratio of r_e/D_h varies monotonically with the experimentally determined R_c* within this contour length regime suggesting a direct relationship between the average position of the LifeAct domains and their ability to crosslink.